Title:	**Performance of Adhesives in Glulam after Short Term Fire Exposure**
Authors:	Hailey Quiquero, York University Bronwyn Chorlton, York University John Gales, York University
Subject:	Fire & Safety
Keyword:	Timber
Publication Date:	2018
Original Publication:	International Journal of High-Rise Buildings Volume 7 Number 4
Paper Type:	1. Book chapter/Part chapter 2. **Journal paper** 3. Conference proceeding 4. Unpublished conference paper 5. Magazine article 6. Unpublished

International Journal of High-Rise Buildings
December 2018, Vol 7, No 4, 299-311
https://doi.org/10.21022/IJHRB.2018.7.4.299

International Journal of
High-Rise Buildings
www.ctbuh-korea.org/ijhrb/index.php

Performance of Adhesives in Glulam after Short Term Fire Exposure

Hailey Quiquero, Bronwyn Chorlton, and John Gales†

York University, Toronto, Canada

Abstract

As engineered timber such as Glulam is seeing increasing use in tall timber buildings, building codes are adapting to allow for this. In order for this material to be used confidently and safely in one of these applications, there is a need to understand the effects that fire can have on an engineered timber structural member. The post–fire resilience aspect of glulam is studied herein. Two sets of experiments are performed to consider the validity of zero strength guidance with respect to short duration fire exposure on thin glulam members. Small scale samples were heated in a cone calorimeter to different fire severities. These samples illustrated significant strength loss but high variability despite controlled quantification of char layers. Large scale samples were heated locally using a controlled fuel fire in shear and moment locations along the length of the beam respectively. Additionally, reduced cross section samples were created by mechanically carving a way an area of cross section equal to the area lost to char on the heated beams. All of the samples were then loaded to failure in four-point (laterally restrained) bending tests. The beams that have been burnt in the shear region were observed as having a reduction in strength of up to 34.5% from the control beams. These test samples displayed relatively little variability, apart from beams that displayed material defects. The suite of testing indicated that zero strength guidance may be under conservative and may require increasing from 7 mm up to as much as 23 mm.

Keywords: Glulam, Radiant heat, Adhesive, Tall timber

1. Introduction

Engineered timber products are structural materials characterized by the union of wood laminae with polymer-based adhesives. Common uses of engineered timber consistently employed in structural design are built-up sections which provide stability, as well as insulation and integrity. Common examples include: Glulam columns and beams and Cross Laminated Timber (CLT) walls and floors. Sample cross sections of these types of engineered timber can be seen in Fig. 1. Canadian practitioner interest in engineered timber has been encouraged by a recent effort to advocate 12 story tall timber construction the National Building Code of Canada (NBCC) for 2020. The code also uses language describing the use of heavy timber construction which is congruent with engineered timber products. The expansion of CSA O86 timber guidance for engineered timber construction has followed. As demonstration projects, some practitioners have begun to build these high-rise timber structures in Canada. However, with the pending code changes, there remains peaked interest from various Canadian practitioners in methods and sufficient background knowledge to design these buildings with confidence. One of the most notable demonstration projects in Vancouver, Canada is known as Brock Commons. It is an exemplar engineered timber structure as it exceeds height limitations using a regional building code. In this building nearly all Glulam and CLT elements were encapsulated with multiple layers of fire rated gypsum board to simplify the fire design (Jeanneret et al., 2017). This procedure allowed the building to meet required fire resistance rating using the additive rules. To the knowledge of the authors, there was no attempt to quantify the degradation of the timber itself as contributing to part of the fire resistance calculation beneath the gypsum board. The fire rating of Brock Commons may be thought as significantly higher once the resistance of the timber itself is considered. The validity of this assessment is multi-faceted and indeed in need of additional research. Following Brock Commons, an exhaustive study of engineered timber compartments using encapsulated CLT has been made publically available by researchers at NIST and NRC (Su et al., 2018). In that study it was identified that a complicated breakdown of adhesives in engineered timber were occurring at high temperatures leading to delamination as well as unique and complicated compartment fire dynamics for exposed timber. Those researchers have advocated that engineered timber adhesives receive more

†Corresponding author: John Gales
Tel: +416-736-2100 (44221)
E-mail: jgales@yorku.ca

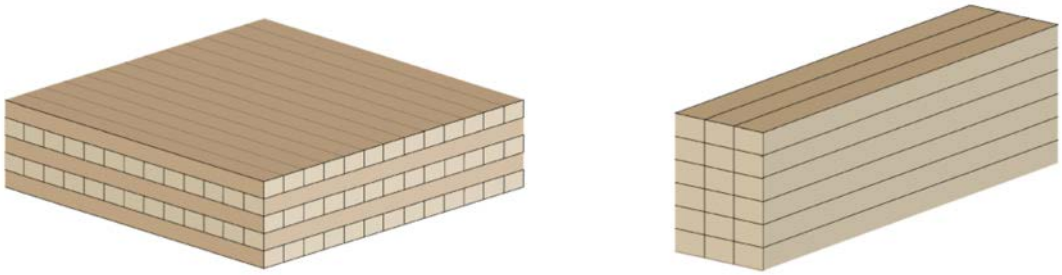

Figure 1. Sample cross section of CLT (left) and Glulam (right). The laminates of CLT vary in direction between each layer while the laminates of Glulam are uniformly in one direction.

research attention.

When exposed to a fire, timber begins to enter pyrolysis and forms a char layer on the exposed surfaces. In the case of engineered timber, other effects such as adhesive degradation also begin to occur and introduce more complex failure mechanisms (see Quiquero et al., 2016). Fig. 2 demonstrates the charring behaviour and heat transfer effects that occur when massive timber elements are exposed to fire. Current guidance allows for a remaining cross-section of the fire-exposed member to be considered "undamaged" below the char and pyrolysis layers. This is typically done by assuming a zero-strength layer beyond the char front, which is meant to implicitly account for degradation effects that include the break-down of adhesive, loss of moisture and pyrolysis of wood. Therefore, guidance does exist to permit un-encapsulated timber from a stability perspective. However, this guidance is in need of review as the current quantification of the zero-strength layer has been debated in recent literature, ranging from 7 to 16 mm depending on the type of fire and the severity (Lange et al., 2015; Gales et al., 2018).

The ability to expose a building's engineered timber is architecturally desirable and therefore studying adhesive breakdown, given documented uncertainty, is of use and indeed a novel contribution. In order for engineered timber to be defensibly left exposed, a greater understanding of the underlying thermal-mechanical properties is required. The study herein addresses this need. To focus the study, the authors predominately considered the after-fire performance of Glulam adhesive as the subject of investigation. The role of Glulam as the primary stability mechanism of most tall timber structures renders intimate knowledge of its behaviour highly important. Currently, there are limited studies available that investigate the severity of adhesive degradation within Glulam. Other types of engineered timber such as CLT have numerous studies examining the effect of fire on their adhesives where they identified that fall off criterion is a critical issue with adhesives (see Emberly et al., 2016; Su et al., 2018). There is a dearth of research attention for all engineered products that address strength of the layer after fire. Studying this aspect may lead to a further understanding of the load

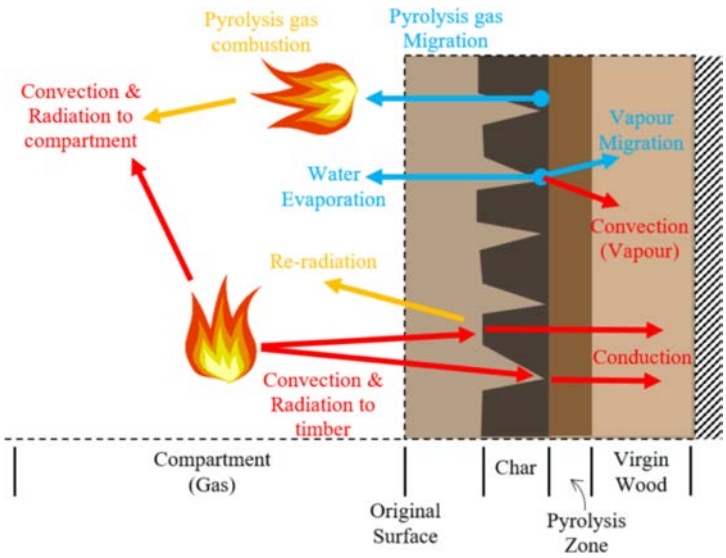

Figure 2. Massive timber charring behaviour and response to fire exposure.

carrying capabilities of the non-charred wood regions of engineered timber, as opposed to regular heavy timber members used as primary load bearing members. As Glulam may be primary load bearing members, often with smaller laminates than CLT but still similar adhesive, this has created a research need to study Glulam as the adhesive layers may be more readily exposed to elevated temperatures where they rely on the adhesive for strength in particular. CLT and other engineered timber products rely on similar adhesives, so some conclusions herein may extend to such other products. The post-fire performance gives indication to the degree of reparability after a fire, which helps provide confidence to authorities having jurisdiction in approving this construction type. Future work is to follow that will specifically consider the in-fire performance. While this study explicitly considers Canadian design context, as the materials tested are provided by local manufacturers, its results are generally applicable to other jurisdictions that are also developing tall timber guidance. The research herein should not be construed as an attempt to establish fire resistance metrics or comparators to ISO / ASTM standard fire exposures. The study herein is attempting to consider the fire resilience of glulam by studying the underlying degradation breakdown of complicated engineered adhesive polymers in two equally important test phases. Phase 1 and 2 deal with explicit and conservative approximation of the zero strength layer at two different scales. Additionally, the small scale experiments focus directly on the specific adhesive performance while the larger scale tests introduce effects such as combined loading and material defects which may influence the failure of the specimens. Next steps that are required for renewed guidance for tall timber structures in fire concludes this paper.

2. Background on Adhesive Degradation

The behaviour of wood in fire is well known and highly predictable based on decades of experiments on the subject. However, the introduction of adhesive introduces highly complex mechanisms that are still in need of study. In particular, the way the adhesive interacts with the char layer and the adhesive degradation itself has scarcely been investigated in realistic building fire configurations.

2.1. Charring Behaviour of Engineered Timber

Engineered timber products are largely believed to char in much the same way that solid timber would. Under extreme heating, wood begins to undergo a process known as pyrolysis around 100°C as its chemical properties begin to change. The wood strength begins to degrade until 300°C which is recognised as the charring temperature of wood, at which point the pyrolysis process has completed and the wood is completely converted to char. After this point, char may continue to develop as the wood behind the char layer is heated, and the exposed char continues to oxidize until it begins to crack and flake off, or is fully consumed. Although the charring rate is realistically a transient property depending on the degree of char that has already formed and the amount of heat exposure, standardized constant charring rates have been developed. For example, a commonly quoted value for Spruce-Pine-Fir (SPF) Glulam is 0.7 mm/min. This rate is meant to encompass the initial rapid char phase while fresh wood builds up an insulating layer of char which then slows the charring rate to a much lower value. However, it has also been derived from standard fire exposure so questions of relevance have been raised. Modified charring rates for Eurocode parametric fires have been proposed (Hopkin, 2016). The codes typically prescribe an additional zero-strength layer of 7 mm beyond the char depth that accounts for the loss of strength in the pyrolysis zone of the heated timber. An in-depth study was done by Lange et al. (2015) in which numerous engineered timber beams were loaded in furnace tests exposed to standard and parametric fires. That research suggested that this layer may range from 8 mm for a short, intense fire, up to 16 mm for a longer fire or standard fire exposure. Another phenomenon which has been observed in engineered timber is delamination, which is the separating of a wood layer from an adjacent one due to the failure of the adhesive. Delamination occurs when thermal penetration into the timber material interacts with an adhesive bondline. The occurrence has been observed most specifically with CLT, due to the comparatively large weight of the lamellae and surface of exposed timber (see Su et al., 2018). There have been numerous studies on delamination in compartment fires but the occurrence of the phenomenon is variable. One study was able to show that in some cases, the delamination timing lined up with the char front reaching the first adhesive bondline (Hadden et al., 2017). That study also suggested that delamination occurred when the char front had not yet reached the bondline, and the adhesive would have been at a much lower temperature than 300°C when it lost enough strength for the lamella to delaminate. Another study by NIST/NRC showed that CLT walls and ceilings began to delaminate variably before and after the char layer had reached the adhesive layers (Su et al., 2018).

2.2. Timber Adhesive Standards

A wide range of standards are currently required for high-temperature performance of adhesive in engineered timber. Fig. 3 shows a summary of timber adhesive standards in Canada from Quiquero and Gales (2017).

These standards (summarized in Fig. 3) are highly fragmented and do not necessarily test conditions that adhesive bonds in timber would be exposed to in a real fire. For example, no standard exists that evaluates the performance of adhesive bondlines beneath the char layer in burnt engineered timber samples, but rather test the strength of the adhesive under uniform heating less than the charring temperature of wood. The main test method for eval-

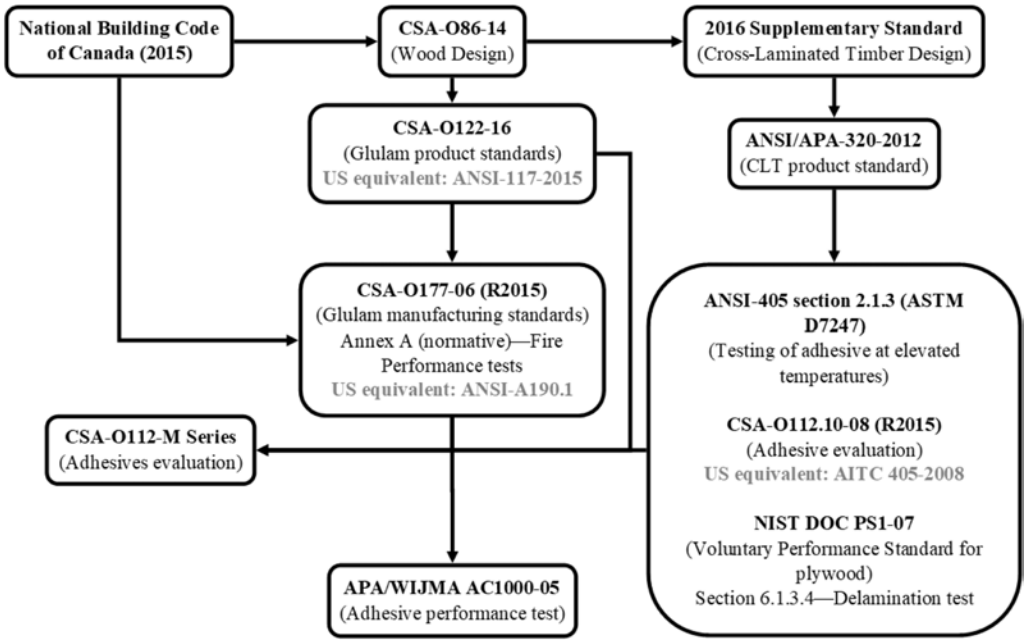

Figure 3. Canadian timber adhesives standards summary (see Quiquero and Gales, 2017).

uating the strength of adhesives in these standards is a shear test by compression loading on specimens that are 50 mm squared by 40 mm thick, with a slight offset on either side of the shear plane.

2.3. Research on Timber Adhesive Fire Performance

No previous tests have been done, to the knowledge of the author, where timber adhesive samples being tested have been exposed to extreme heat and the char front has impinged on the glue line under examination. Adhesives in timber are typically tested at these temperatures below 300°C as the strength of the material is assumed to be completely lost at this point as the wood chars. However, this means that the performance of the adhesive just beyond a char front has not been studied. Notable studies include a study by Frangi et al. (2004) and Clauß et al. (2011). Frangi et al. (2004) tested small 40 mm bond lines on double lap specimens through compression loading for several different adhesives including one phenol-resorcinol-formaldehyde resin (PRF) and five different polyurethane adhesives (PUR). Hundreds of samples were heated in an oven to various temperatures ranging from ambient to 170°C. It was found that the behaviour of the PUR varied greatly between manufacturer and thus chemical composition. Three PUR and the PRF adhesive performed similarly to that of the wood itself, while two of the PUR performed very poorly and began to lose strength from 50~70°C. Clauß et al. (2011) similarly performed shear tests on several different adhesives but using single lap samples with bond lengths of only 10 mm through tensile loading. The specimens were uniformly heated to various temperatures up to 220°C. The results in this test series were highly variable, but similarly found that the performance of various PUR adhesives were diverse with some losing thermal stability around 70°C while others remained stable until 150~200°C. The most recent testing that specifically referenced to adhesive performance was a two-part test series by Nicolaidis et al. (2016) and Emberley et al. (2016) on glued single lap samples exposed to environmental chamber heating and CLT beams exposed to radiant heating, respectively. Pine and spruce wood were used, respectively, with a one-component PUR. The single lap samples had 600 mm bond lengths and were heated uniformly immediately prior to testing. The exposure on the CLT beams was akin to a realistic fire condition but at a very low heat flux of 6 kW/m^2, thus inducing a gradient of in-depth temperature below the pyrolysis temperature of wood. The bond lines were mostly uniformly heated perpendicular to the bond on the tension side of the CLT beam, increasing the temperature of the bond lines to just 60~85°C. Heating perpendicular to the bond line is a common scenario on CLT in realistic compartments, however Glulam members will often experience heating parallel to the exposed adhesive lines. In both parts of that experimental series, changes in the failure mode from primarily timber failures to primarily adhesive failures were seen in the higher temperature range tests. Of particular note, the failure modes in the adhesive were often made more severe by the discontinuity and stress concentrations caused by timber failure propagating into an adhesive joint. This stresses the importance of the size effect in experiments and failure modes changing based on the length of bond line tested. An experimental programme was previously undertaken by the authors to research the

underlying mechanics of the failure of fire-damaged engineered timber, specifically in timber box sections. The test series included axial compression of glulam coupons and four-point loading of short glulam beam sections (Quiquero and Gales, 2016; Quiquero et al., 2016). A group of the samples were burned in a furnace in a one hour standard fire, and allowed to burnout after fuel supply was halted for an additional hour. Following this the samples were allowed to cool, and tested at a later date so that the material could reacclimatize in moisture and so that the mechanics of the beam performance and failure could be closely studied. Of the samples that were not burnt, some were left as control specimens with original dimensions and a portion were manually altered to carve off the corresponding char depth to the burnt specimens. Specimens were carved to remove the char depth recorded in order to investigate whether the assumption that the cross-section below the pyrolysis zone had full strength. In all cases in which a corresponding specimen was carved to match a burnt specimen, the manually reduced test always had a significantly higher capacity than the burnt counterpart. This indicated that there was some other factor contributing to the failure of the specimens other than the loss of cross-sectional area. The adhesive in the engineered timber could be affected by the extreme heating and the charring encroaching on glue-lines, causing it to have a reduced strength. Samples were not of representative length (1 m). The study herein considers a realistically sized member, and controlled study of the strength of the adhesive layer.

3. Methodology

A holistic test programme is presented to study commercially available glulam and the performance of adhesive after exposure to fire conditions. The Glulam had 5% moisture content (before heating). It was machine rated as 24f-ES and made of SPF species. Two test phases were considered generalized by the experimental goal. For Phase 1, Glulam samples of 100 by 100 by 45 mm were utilised (scaled to fit a heating apparatus). For Phase 2, Glulam samples were beams of dimensions 4200 by 195 by 45 mm. As such, the timber members considered were thin, and only moderate degrees of charring were considered.

In order to create a shear test setup compatible with the sample dimension requirements for the cone calorimeter, a shear apparatus was built (see Fig. 4). The apparatus was placed between two loading plates on an INSTRON load actuator through which the wood blocks were placed under a shear force through compression loading. The loading rate was 1 mm/min. The shear plane was along the centreline of the wood specimen that corresponded to the adhesive bond to be tested, shown in Fig. 4. Slip was measured using Digital Image Correlation (described below). The failure mode is expected to be due to primarily to shearing stresses.

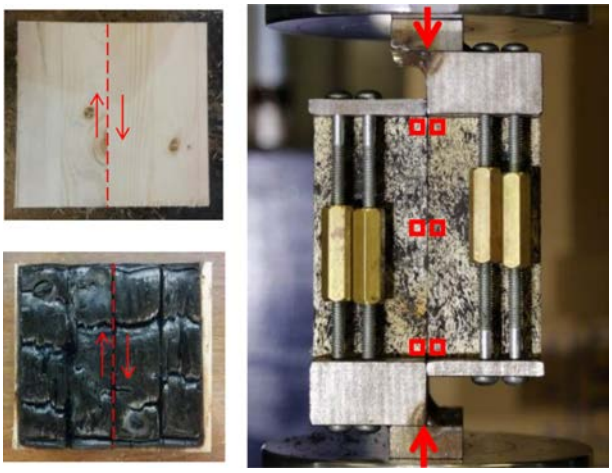

Figure 4. Shear plane shown on unheated and heated samples (left) and shear apparatus test setup (right).

Five identical Glulam beams were charred at different locations along the beam for the full duration of the fire. An additional four beams consisted of control samples and samples that would be carved to simulate charring for a total of 9 beam tests: 2 Charred and 1 Carved Mid-span; 3 Charred and 1 Carved in a side region; and 2 Control. All burnt beams were exposed on two sides along the depth of the beam in the desired charring region to provide a relatively consistent char depth. Two beams were charred directly in the center of the beam, and three were charred on one end, 270 mm from the edge of the beam (Fig. 5). This heating configuration had negligible differences in the amount of char observed (5 +/- 1 mm at three locations on each beam equally spaced and across the depth). The heating configuration was determined through

Table 1. Summary of the number of samples tested for each adhesive type, heat exposure and heating duration

Heating duration (min)	Number of PUR samples with each heat flux exposure		Number of PRF samples with each heat flux exposure	
	30 kW/m^2	50 kW/m^2	30 kW/m^2	50 kW/m^2
0	5		5	
3	3	2	3	2
6	3	2	2	2
10	4	4	2	3
15	4	3	2	2

Figure 5. Test setup of the heating portion of the experiment for the moment region (left) and the shear region (right).

a series of test burns. The charring locations were chosen to give varied results in the loading part of the testing; where damaged shear and moment regions of the beam could be studied separately – hence the beams were not heated uniformly. Aluminum foil was wrapped around the beam immediately adjacent to the intended char zone to limit the radiant heat and flame spread to other parts of the beam. When the pool fire burned out, the beams were left to self-extinguish. Since this happened immediately, no water was used. The beams were then flipped and the heating was repeated for the other side. This test setup allowed for two-sided heat exposure, a notable difference from the one-way heating performed on the small scale tests. An area of cross section equivalent to the charred area on the five beams that underwent the fire testing was removed from two of the non-charred beams to facilitate comparison of strength of the beams. The area removed was approximately 5 mm deep on all four exposed sides and 1 m long, in the same locations as were charred during the fire tests (either in the moment region or the shear region). All beams therefore had the same non-charred cross-sectional area for the mechanical testing. In this manner, any variation in the strength data will be due to factors other than the effective cross section reduction of the charred beams. The intention of this charring degree (5 mm) is not to be thought of as the authors providing information on timber's fire resistance, but rather a controlled set amount of damage that can allow the underlying breakdown mechanisms of timber exposed to fire to be rationally studied. After time for re-acclimatizing to lab moisture conditions, 5%, four-point loading was performed to induce constant moment and shear on the specimens. Beams were restrained against lateral torsion. The loading setup can be seen in Fig. 6.

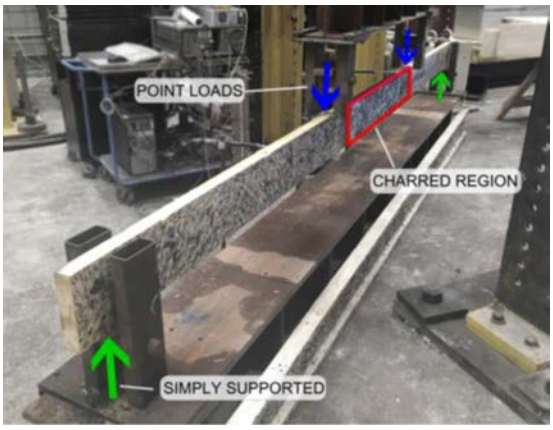

Figure 6. Mechanical loading of simply supported beam with four point loads.

3.3. Deformation Measurement

Digital Image Correlation (DIC) was used to monitor the deformations of all experiments. This has previously proven accurate for measuring displacements and strain in wood specimens (Quiquero and Gales, 2016). The displacement measurement technique uses a pixel-tracking software to locate user-specified locations on a series of high-resolution photographs. A speckled pattern is painted on the surface in order to ensure there is a very unique patch of pixels for the software to track from image to image. The software then records the location of the pixel patch in each photograph, which may be used to compute the displacement and relative deformations. In Phase 1 tests, the slip was measured at 3 points along the shear line. A sample of the pixel patches used to track the slip are shown in the right-hand image in Fig. 4. In Phase 2 tests, the centre point deflection of the beam was measured. This was complemented using linear potentiometers to record out of plane distortion. The pixel-tracking software that was used to process the test images was GeoPIV RG (Stainer, 2015). A Canon Mark III 5D DSLR camera was used in conjunction at 3 second intervals.

4. Results

The results of the fire exposure and subsequent mechanical loading of the Glulam specimens are discussed below for Phases 1 and 2.

4.1. Phase 1: Small scale adhesive shear tests

The resulting char quantifications show predictable results however, the mechanical results had high variance between the repeated samples. This is expected due to the natural complexity and non-homogeny of wood and the small size of the samples tested.

4.1.1. Post-fire damage state

For the 30 kW/m^2 incident heat flux exposure, flaming ignition was not seen in the majority of the samples. Rather, smouldering was observed without flaming. For the 50 kW/m^2 incident heat flux exposure, flaming ignition in all samples was seen after around 30-40 seconds of exposure. After the samples were broken in half by shear

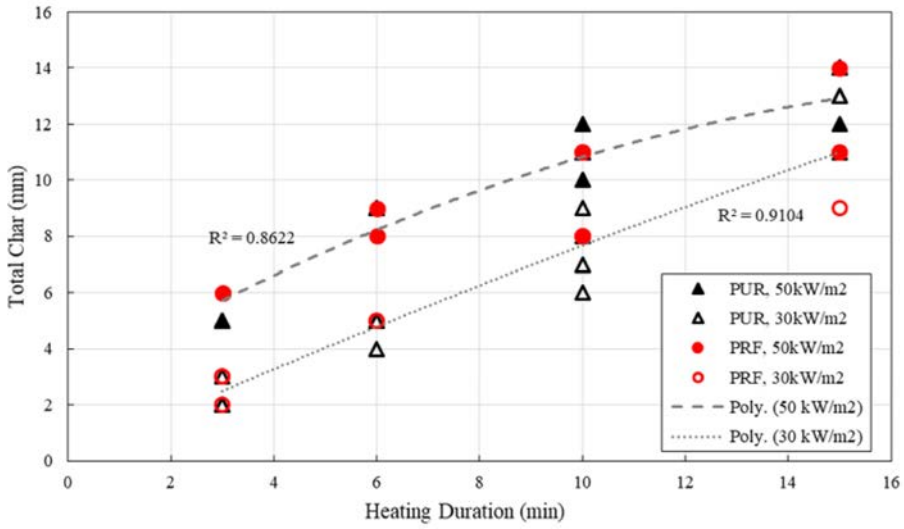

Figure 7. Total char depths measured on samples versus the heating duration.

testing, the average char depth at the centreline was also measured. The char depth was taken as the average of three points along the centreline (typically 1 mm of each other). The char depths of each sample versus their heating durations is plotted in Fig. 7. It can be observed that the char depths for the higher heat exposure were typically higher than those of the lower heat exposure. The trend for both the 50 kW/m^2 and 30 kW/m^2 exposures decreased in slope with longer heating durations, while this is more pronounced in the higher heat exposure. This indicates that the charring rates slow over time, as the char layer builds up and inhibits heat transfer as is expected. The higher heat flux charring rate trend tended to approach the lower heat flux constant rate, around a minimum value of 0.75 mm/min. This indicates that this might be a minimum rate of charring that may be seen in timber above the pyrolysis temperature for these incident heat fluxes. This corresponds well with recommended charring value of 0.7 mm/min for standard fire exposures. Overall, the charring behaviour of the samples was very uniform and predictable. Char depths seen were close to uniform along the surface of the specimens.

4.1.2. Post-fire mechanical behaviour

The primary failure mode of the Glulam was by shear along the adhesive bond line, as intended by the test setup. A typical failure may be seen in Fig. 8. The area beneath the char layer was used to calculate the failure stress of each sample at the peak load reached in the test before failure. If the adhesive within the wood region below the char front of the samples was also unharmed, the failure stress of each sample should be equal (although the peak load would be lower due to loss of cross-sectional area). However, a general decreasing trend in adhesive strength with heating duration was seen. This indicates that the adhesive beyond the char layer is affected by the heat and may have lost some additional strength unaccounted for in the sacrificial char method.

A correlation is made between the remaining shear capacity of the samples and their respective remaining shear area. In theory, if the adhesive held 100% of its strength after heat exposure, these two values would correlate exactly. That is, if a sample had 80% of its shear area left after heating, the remaining shear capacity should be 80%. This is shown as the red dashed line in Fig. 9. Any sample falling below this line represents a sample that did not retain its full adhesive strength – that is, the loss of shear capacity was greater than the loss of area. The figure illustrates a large amount of variance in the capacity of the samples. It can be seen that the majority of the samples fell well under the perfect correlation line, with most samples having a remaining area beneath the char of above

Figure 8. Typical failure mode of shear along an adhesive bond line.

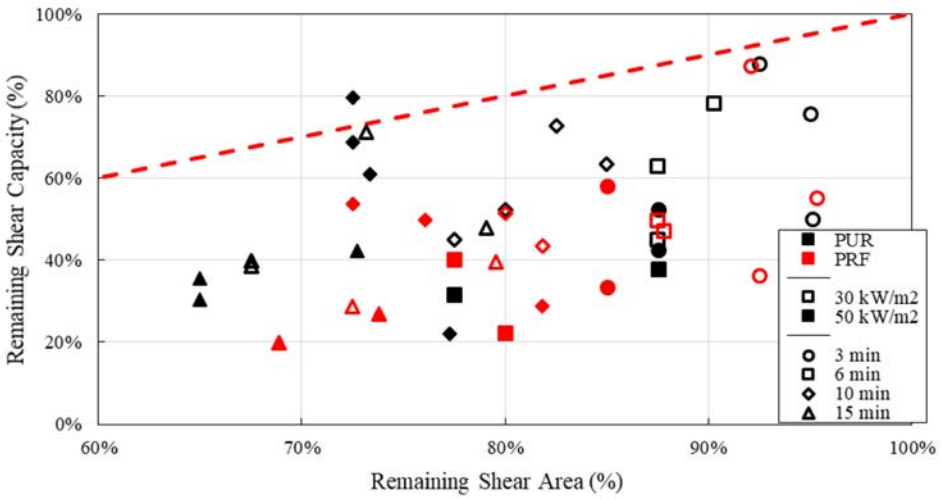

Figure 9. Comparison of remaining shear capacity versus area for all samples.

60%, but many samples falling to as low as 30% remaining capacity. On average, the samples had a remaining capacity 32% below their remaining shear area. Further, the capacity of the PRF samples fell an average of 40% below their remaining area while the PUR samples were 26% below. This could indicate a difference in the adhesives or in the way they were prepared, with the PUR bonds being produced by the manufacturer while the PRF bonds were produced in the lab.

Additionally, from Fig. 9, there is no clear trend or distinction developed within any of the heating durations or exposures, though it is clear that the adhesive performance falls below that of which should be expected. A comparison was made with the remaining capacity that the standard recommended sacrificial charring method would be predicted, using a charring rate of 0.7 mm/min plus a zero-strength layer of 7 mm. It should be noted, however, that these recommended charring rates are not validated for exposures other than a standard-fire, and are thus not totally applicable to a constant heat flux radiant exposure, but are included here for comparison (as it was observed to closely correlate to that seen for a 50 kw/m^2 exposure as stated above). As seen in Fig. 10, when compared with the actual remaining shear capacity, the standard's predictions still fall significantly below the correlation line. This new data set is plotted in grey in Fig. 10 compared to the original data set in black. There may be two possible causes for the reduced strength of the samples. The first is that, due to the small thickness of the samples, all of the adhesive beyond the char layer may be reduced in strength by a certain percentage corresponding to the lower capacities mentioned above. However, since the adhesives must have been tested to the standards discussed earlier in the manuscript, the adhesive should retain full strength for temperatures below the charring temperature of wood. Secondly, the adhesive may be full strength at a certain depth beyond the char layer, but an additional layer of adhesive beyond the encroached char front may have been degraded. In other words, a larger zero-strength layer may be present than is recommended in standards. It is likely that the adhesive and therefore the combined strength of the engineered wood product may have degraded to a certain depth beyond the char front, after which the remaining adhesive there may be assumed to have full strength. This effect is investigated further below.

Another factor that may contribute is the loss of strength of the wood above 100°C, as many of the failures were a combination of wood and adhesive failure. If the adhesive is assumed to have full strength at a certain depth beneath the char layer, then the area of that full strength zone may be computed using the peak shear capacity of each sample. It was assumed that this full-strength zone spans the full height of the samples, and that the width is measured through the thickness of the sample from the unheated face. In this way, the penetration of the zero-strength zone may be calculated and compared with the char layer measurement. On average, the zero-strength layer penetrated 13.3 mm beyond the base of the char zone. Separated for each adhesive, this value was an additional 16.2 mm for the PRF samples and 10.7 mm for the PUR samples. As a comparison, 16 mm was added to the measured char depth of each sample and a new remaining shear area was calculated. This new data set may also be compared to the original and standard-predicted data sets in red in Fig. 10. It can be seen that increasing the zero-strength zone to 16 mm below the measured char depth of the samples results in a much better prediction of the remaining strength, with the majority of the samples falling over the line. A more conservative value of 23 mm below the char depth could be used to give a 95th percentile of samples falling above the line, which is shown as the blue series in Fig. 10. The samples tested were very small scale, so larger

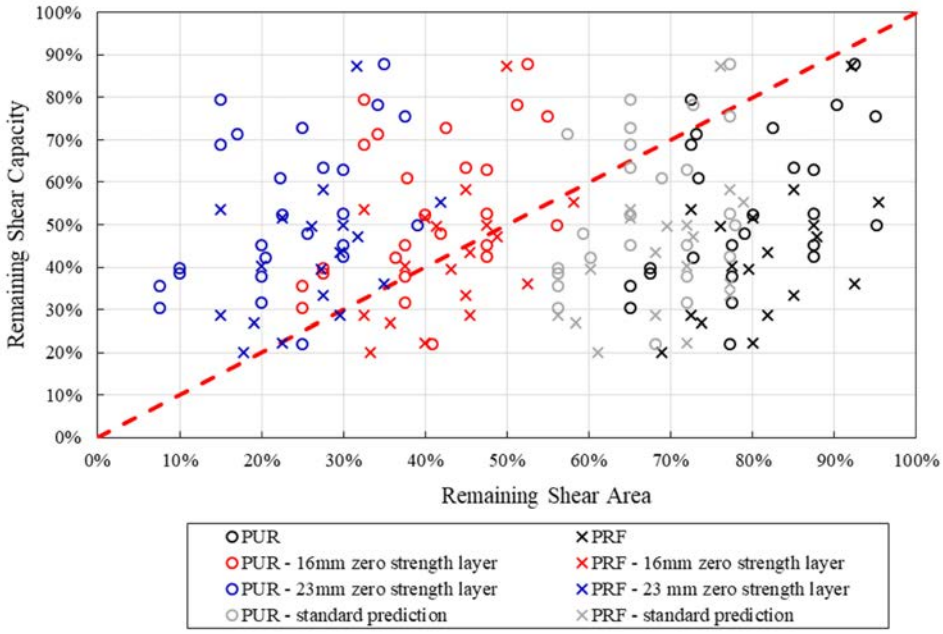

Figure 10. Remaining shear capacity of samples versus different predictions of actual remaining shear area at full adhesive strength, compared with the measured char depths and the standard predicted sacrificial char method.

scale members should be tested. A greater area of unheated wood behind the char layer would likely increase the remaining capacity of the wood so such a drastic addition to the zero-strength layer may not be required. Additionally, effects introduced by cracks propagating into the adhesive layer and introducing stress concentrations has been found in the past to be a large influence on adhesive failure and cannot be ignored. In addition to the strength performance of the specimens, digital image correlation was used to record the displacements during loading. The slip was calculated using the procedures outlined earlier and was averaged over the three measurement locations to represent the average slip of the adhesive line. A comparison is made between the load-slip behaviour of several representative samples under 50 kW/m^2 incident heat exposure with PUR and PRF adhesives in Fig. 11. It is clearly observed in the figure that as the heating duration increased, lower loads were reached for the same level of slip. This indicates that the adhesive stiffness or rigidity has degraded over increased periods of heating.

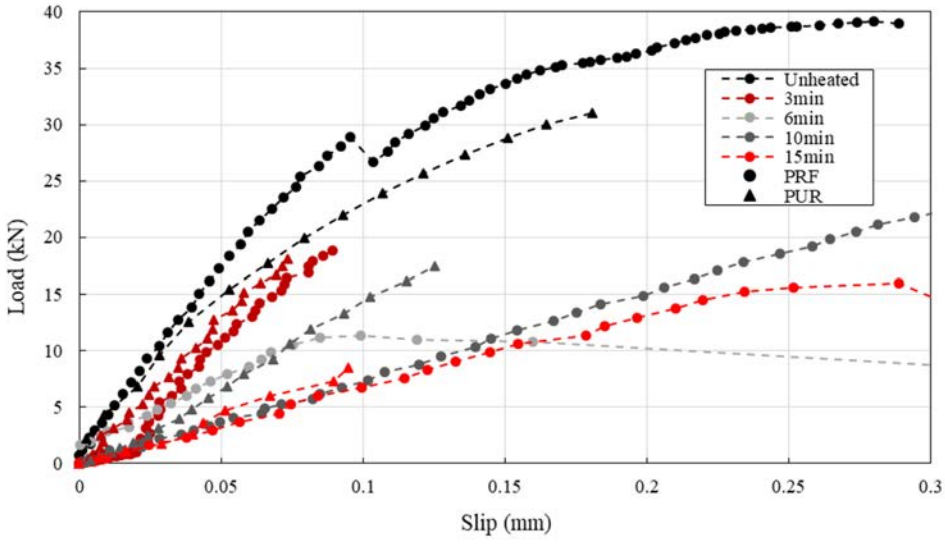

Figure 11. Load versus slip behaviour for heated for different durations under a 50 kW/m^2 incident heat flux.

Figure 12. Failure mode of a Glulam undamaged control beam, whose failure originated along the adhesive bond lines within the moment region.

4.2. Phase 2: Large scale beam bending tests

The resulting flaming behaviour and charring of the burnt beams was consistent through all five exposed samples. Variability cannot be quantified in this phase as a smaller number of beams were tested due to the larger scale. However, the results of the burnt beams are compared herein to the unaltered control beams of original dimensions and two beams with manually reduced cross-sections in critical regions.

4.2.1. Post-fire damage state

To adequately quantify the degree of charring so that the samples could be adequately carved, the charred and damaged samples were tested first in four-point bending. After testing, the beams were then sliced in the burnt region and the charring depths were measured across the cross section (5 +/- 1 mm), where it was confirmed that there were minimal differences in the char depths observed. 5 mm was used for the depth of all carving on the sides of the beams. Carving was performed manually through a plane process and confirmed afterwards.

4.2.2. Post-fire mechanical behaviour

As they were mechanically loaded, the beams primarily failed within the moment region, along both adhesive bond lines and finger joints. The failure mode can be seen in Fig. 12.

The average failure loads obtained during the mechanical loading are summarized in Fig. 13. On an average basis, the control beams failed at the highest applied load, with all of the carved and charred beams failing at lower loads. All failure loads were higher than the hand calculated estimated strength, accounting for only the reduction in cross sectional area (predicted as 10.6 kN). The displacement of the beams is presented in the plots of load versus vertical displacement in Fig. 14. Displacements were measured by digital image correlation. In all tests lateral movement, by linear potentiometers (an indication of torsional failure) was negligible.

The two control beams failed at relatively high loads with the difference possibly due to inherent material variability between the two specimens. Amongst beams damaged in the moment region (midspan), the results were quite variable; the beam with mechanically reduced cross section failed at a relatively low load compared to the charred specimens, which withstood relatively high loads, losing only 8.9% (1.9 kN) of their capacity. It is possible that the carved beam had a material defect that was not visibly apparent, causing the low failure load. A large reduction in moment capacity was not expected from the exposure as the depth of the cross-section was largely unaltered, contributing to most of the moment capacity. Regarding beams damaged in the shear region, the beam that had its cross section mechanically reduced through carving displayed the highest stiffness, as the slope of its load-displacement curve is the greatest, and experienced a higher failure load than any of the charred beams. The beams burnt in the shear region failed at relatively low yet consistent values of load, while the mechanically carved beam performed better, and failed at a higher load. The CSA O86-14 guidance predicts a failure load of 10.6 kN for a cross section reduced by 5 mm on two sides of the beam (which is the damage state that was observed). All of the shear damaged beams observed a higher failure load than this prediction. The charred beams failed on average at a load 24.6% lower than the beam that has been mechanically carved in the shear region. Since the beams that were damaged through charring had the same

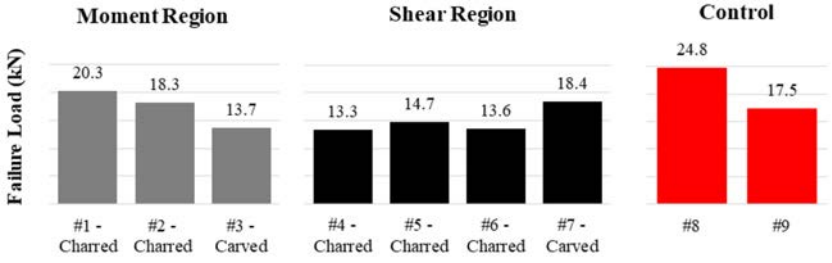

Figure 13. Failure load of all beams damaged in the moment region, shear region, as well as the control beams.

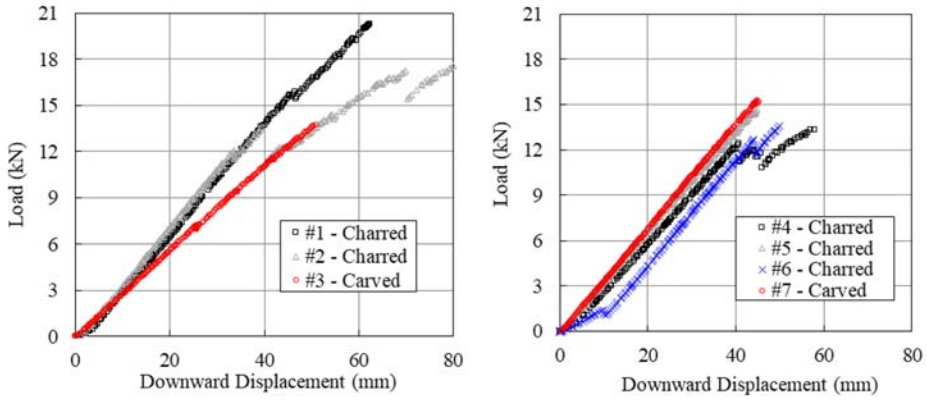

Figure 14. Load versus downward displacement beams damaged in the moment region (left) and shear region (right).

cross section as the beams that were damaged through mechanical carving, this difference is indicative of adhesive degradation. This is in line with the loss of strength observed in Phase 1 of the testing and the previous research discussed in Section 2.3. To achieve a predicted failure load for the charred beams 24.6% lower than the predicted load of the carved beam, the equivalent cross section of the beam would be reduced further by 4.3 mm on both sides (beyond the reduced dimensions of the carved beam). This reduction in area would be considered to be due to degradation effects (that is, a zero strength layer), as the char depth has already been accounted for in the reduction in area of the carved beam. Continuing to examine the beams charred in the shear region, the burnt beams failed at a load 34.5% lower than the control beams. A reduction in cross sectional area of 7.8 mm on two sides of the beam would be required to generate a predicted value 34.5% lower than the predicted failure load of the undamaged beams. Examining standard allowances, and in particular CSA O86-14, the amount of cross sectional area lost to charring and other effects is calculated first by determining the char depth, and then adding allowances for the zero strength layer. The remaining area is assumed to retain its full, initial strength. Annex B.4.2 in CSA 086-14 quantifies the rate of char of Glulam as 0.70 mm/min, indicating that at five minutes of exposure the char depth would be calculated as 3.5 mm. As previously mentioned, this standard guidance is not entirely applicable to beams damaged as per the procedure used for these tests, but for comparison purposes is still considered. In addition to the calculated char depth, Annex B.5 quantifies the zero strength layer for exposure times less than 20 minutes as being interpolated linearly between 0 mm and 7 mm, depending on the time exposed. At five minutes of exposure, this would predict the zero strength layer as being 1.75 mm, meaning that the total calculated depth lost due to char and the zero strength layer would be 5.25 mm. In order to create a loss of depth of 7.8 mm, the zero strength layer would need to be calculated as 4.3 mm rather than 1.75 mm (assuming the predicted char depth is correct). This value of 4.3 mm, which would be considered to be due to degradation effects, is the same depth that has been found to be compromised in the comparison of the charred and carved shear region beams. To achieve a zero strength layer of 4.3 mm, the depth of the zero strength layer must be interpolated linearly between 0 mm and 17.2 mm rather than 7 mm (for exposure times less than 20 minutes). This suggested value of 17.2 mm implies that the depth of the zero-strength layer proposed (23 mm past the char depth) would be a conservative value when applied to these large-scale beams.

5. Future Research

In Canada, heavy timber construction is permitted currently in mid-rise buildings by code and larger structures are already planned to having prescriptive code approval. However, with heavy timber construction comes large Glulam (or other engineered timber) structural elements which have the potential to be exposed to fire in an extreme scenario. In larger members, it has been seen in previous research that material defects or timber cracks propagating into adhesive lines have significant potential to govern the critical failure of these elements. The stress concentrations from these defects has been observed to induce delamination of adhesive layers in heated engineered timber and is of the utmost importance to be studied in the near future.

There is one significant difference when considering Phase 1 and Phase 2. Phase 1 had significant water suppression opposed to Phase 2 that had none. The authors believe that this fact is plausibly responsible for the differences observed in the zero strength calculations and this aspect requires additional study. There is no question in a real fire water will be utilised to suppress a fire in a timber building (exposed or not) and this can complicate the degree of damage to adhesives that are in a liquid state, and may re-solidify during the cooling process. Neverthe-

less, the large scale beams do yield confidence that for short term exposures without water suppression, the adhesive degradation will be of minor effect in comparison to the small scale samples with short term heat exposure and with water suppression. Further testing to investigate the influence of the water suppression on the results should be done.

While self-extinguishment was observed in the beam samples, it will be necessary to study this phenomenon to a greater degree where fire spread is allowed. A comprehensive listing of future research needs for enabling high rise timber beyond adhesive degradation is provided in Jeanneret et al. (2017).

To study the effect of longer term exposure it is necessary to scale the cross-sections up to representative sizes for mass timber (min of 190 mm × 190 mm). This will also allow discussion into real specimen section behaviour and direct conclusions may be drawn about realistic performance. Until these tests are performed there is legitimate concern in the authors' opinion that a prescriptive rate for the zero strength layer criterion of 7 mm for engineered Glulam may not necessarily be conservative. These future tests may allow a conclusive solution or criterion to be drawn, however for now a range should be expected that depends on more factors than just the type of heating as discussed in other literature. Factors including member size, adhesive composition, heating duration and exposure should be considered for all types of engineered timber.

While the work done herein has been compared to prescriptive code methods of predicting the capacity of heavy timber structural elements in fire, the suggested increase in zero strength layer is drastic and likely largely over-conservative. The results have shown, however, that the behaviour is so variable and highly complex that a very conservative prescriptive approach would be required. However, finite element modelling of timber proponents may be used to more accurately predict the behaviour of such components if an appropriate model is used. Computer modelling and analysis should be developed and validated incorporating the effects of these findings in order to accurately predict the behaviour of complex engineered timber structures.

It should also be noted that the authors only considered one type of adhesive in manufactured Glulam, along with their own lab grade adhesive. Additional adhesives by various manufactures and of different compositions should also be considered, and it should be recognized that there currently is significant research being performed into advancing adhesives so that they do not degrade to the same degree in high temperatures seen in fires. The smaller scale samples would be highly influenced by any small defects or gaps within the adhesive layers, the critical effects of which would be amplified. This was seen as the effect was less in the larger beams tested and should be investigated further with more repeated tests and different adhesives.

6. Conclusions

Due to the drivers towards massive engineered timber construction in Canada as of late, it is paramount to delve deep into the details of the material's performance in and after fire scenarios. Studying the material post-fire damage (as opposed to in-fire) allows details in the mechanics of the material's behaviour and failure to be observed. Additionally, the resilience of massive timber post-fire is an important topic to be discussed. The opportunity to have the capability to build with and understand materials that are resilient to fire and how to rehabilitate and reuse the structures after such an event also holds immense merit in the realm of property value, business continuity and insurance. If Canada is to build exemplar structures with engineered timber exposed, having confidence in having the material exposed is invaluable.

In the small scale testing, although the high variance in the results typical of wood was seen, some clear trends emerged in the strength and slip properties of the adhesive with varying heat exposures. A clear downwards trend was seen in the strength of all adhesive samples when plotted against heating duration, both for the 30 kW/m^2 and the 50 kW/m^2 heating regimes. By only considering the charred layer or the sacrificial char layer from recommendations, the remaining full-strength zone and thus the predicted remaining capacity of all specimens was greatly over-estimated. On average, an added zero strength layer of 16 mm beyond the recorded char depth was required, with a conservative 95th percentile zero strength layer being 23 mm beyond the char front. The slip behaviour also exhibited trends of increased slip with load on the samples. This indicates that the heated adhesive loses some stiffness compared to the unheated samples.

In regards to the beam testing, charring reduced the strength of the beams when compared to the control samples. The moment damaged beams had their capacity reduced by only 1.8 kN (on average) in comparison to the control beams. This relatively small reduction in strength between the control beams and the charred beams should be expected, as the beams were charred on their long side, but tested in bending standing vertically. Bending is more impacted by depth and section modulus, while shear is more impacted by cross-sectional area. Material defects may have played a role in the variability of the beam carved in the moment region. The beams charred in the shear region had their capacity reduced by an average of 7.2 kN compared to the control beams and 4.5 kN compared to the carved beam, which are significantly larger reductions in strength compared to the moment damaged beams. In all instances, the beams failed at a higher load than directly predicted by current guidance, in particular CSA O86-14 equations for Glulam. However, in examining reduction in strength of the charred shear region beams in comparison to the carved beam, the determination of the zero-strength layer may not fully account for all degradation effects that

are occurring.

Both the small scale and large scale testing showed that the current guidance that exists for approximating the zero strength layer (7 mm), may in some instances be under conservative. These may be effected by suppression operations along with fire type and duration, and the size and defects of the specimens. It is recommended by the authors, that until a more holistic database of tests is established, conservative approximations be used in calculations involving exposed engineered timber with adhesives (23 mm).

Acknowledgments

NSERC discovery grant. The authors thank Chloe Jeanneret, Georgette Harun, Beth Weckman, and Matt Smith for their previous contributions.

References

CSA O86-14. (2016). Engineering design in wood, CSA Group, Mississauga, Canada.

DiDomizio, M. J., Mulherin, P., and Weckman, E. J. (2016). "Ignition of wood under time-varying radiant exposures." Fire Safety Journal 82. 131-144.

Emberley, R., Nicolaidis, A., Fernando, D., Torero, J. L. (2016). "Changing Failure Modes of Cross-Laminated Timber." Structures in Fire, Proceedings of the 9th international conference, New Jersey, USA. 643-649.

Frangi, A., Fontana, M. and Mischler, A. (2004). "Shear behaviour of bond lines in glued laminated timber beams at high temperatures." Wood Science and Technology 38. 119-126. doi:10.1007/s00226-004-0223-y

Gales, J., Zhou, A., Smith M., Braxton, N., Smith, C., and LaMalva, K. (2018). Chapter 11: Acceptance Criterion, Structural Fire Engineering Manual of Practice, ASCE, Virginia, USA. 15 pp.

Hadden, R. M., Bartlett, A. I., Hidalgo, J. P., Santamaria, S., Wiesner, F., Bisby, L. A., Deeny, S., Lane, B. (2017). "Effects of exposed cross laminated timber on compartment fire dynamics." Fire Safety Journal 91. 480-489.

Hopkin, D., Schmid, J., Friquin, K. (2016). "Timber Structures Subject to Non-Standard Fire Exposure – Advances and Challenges." WCTE. 12 pp.

Jeanneret, C., Smith, M., and Gales, J. (2017). "Fire safety towards enabling timber structures in Canada." Applications of Structural Fire Engineering.

Lange, D., Boström, L., Schmid, J., Albrektsson, J. (2015). "The Reduced Cross Section Method Applied to Glulam Timber Exposed to Non-standard Fire Curves." Fire Technology 51. 1311-1340. doi:10.1007/s10694-015-0485-y

National Research Council of Canada, Canadian Commission on Building and Fire Codes. (2015). National Building Code of Canada, National Research Council of Canada, Ottawa, ON.

Nicolaidis, A., Emberley, R., Fernando, D., Torero, J. L. (2016). "Thermally Driven Failure Mode Changes in Bonded Timber Joints." Proceedings of World Conference on Timber Engineering, WCTE 2016, Vienna, Austria.

Quiquero, H., Gales, J., and Hadjisophocleous, G. (2016). "Behaviour of Char Layer in Fire-Damaged Box Section Timber Beams." Interflam 2016. 1063-1074.

Quiquero, H. and Gales, J. (2017). "Comparing timber adhesive shear strength properties after fire damage." Fire and Materials, California, USA. 556-566.

Reszka, P. and Torero, J. L. (2008). "In-depth temperature measurements in wood exposed to intense radiant energy," Experimental Thermal and Fluid Science 32. 1405-1411. doi:10.1016/j.expthermflusci.2007.11.014

Spearpoint, M. J. and Quintiere, J. G. (2001). "Predicting the piloted ignition of wood in the cone calorimeter using an integral model - effect of species, grain orientation and heat flux." Fire Safety Journal 36. 391-415.

Stanier, S.A., Blaber, J., Take, W.A. and White, D.J. (2015). "Improved image-based deformation measurement for geotechnical applications." Canadian Geotechnical Journal, 53(5): 727-739

Su J., Lafrance P.S., Hoehler M., and Bundy M. (2018). Fire Safety Challenges of Tall Wood Buildings – Phase 2: Task 2 & 3 – Cross Laminated Timber Compartment Fire Tests. FPRF. 397 pp.

Yang, J. C. et al. (2015). International R&D Roadmap for Fire Resistance of Structures: Summary of NIST/CIB Workshop, National Institute of Standards and Technology, Maryland, USA.